

Received January 13, 2020, accepted January 28, 2020, date of publication February 5, 2020, date of current version February 13, 2020.

Digital Object Identifier 10.1109/ACCESS.2020.2971777

Robust Repetitive Learning-Based Trajectory Tracking Control for a Leg Exoskeleton Driven by Hybrid Hydraulic System

YONG YANG¹, XIUCHENG DONG¹, XIA LIU¹, AND DEQING HUANG², (Member, IEEE)

¹School of Electrical Engineering and Electronic Information, Xihua University, Chengdu 610039, China

²School of Electrical Engineering, Southwest Jiaotong University, Chengdu 611756, China

Corresponding authors: Xiucheng Dong (dxc136@163.com) and Deqing Huang (elehd@home.swjtu.edu.cn)

This work was supported in part by the National Natural Science Foundation of China under Grant 61773323, Grant 11872069, and Grant 61973257, in part by the Key Projects of Sichuan Science and Technology Department under Grant 2018JY0463, and in part by the Chunhui Plan of the Chinese Ministry of education under Grant Z2017076 and Grant Z2018087.

ABSTRACT For the purpose of reducing power consumption of a leg exoskeleton for augmenting human performance, a novel hybrid hydraulic system (HHS) which includes a unidirectional servo valve and a solenoid on-off valve is excogitated, and its energy saving control is studied in this paper. Inspired by the varieties of contact force between human leg and ground during walking, the unidirectional servo valve and the solenoid on-off valve are only activated in the stance phase and the swing phase, respectively. In the stance phase, a robust repetitive learning scheme is presented by using the backstepping technique for the unidirectional servo valve, aiming to track the periodic human leg movement, and in the swing phase, an on-off control is proposed for the solenoid valve to release the pressure in the hydraulic cylinder so that the exoskeleton leg is bent by the human leg passively. The proposed control strategy is implemented in an ARM-based embedded microprocessor and the control performance is verified via experiment on the developed exoskeleton robot. The experimental results show that the power consumption of the proposed system is almost 30% less than that of systems with bidirectional hydraulic system.

INDEX TERMS Leg exoskeleton, robust repetitive learning, hybrid hydraulic system, energy saving.

I. INTRODUCTION

Exoskeleton is a wearable robot that can help wearers enhance their physical abilities [1], [2], such as increasing the strength of soldiers [5], assisting the elderly to walk [3], and rehabilitating the patients with limb injuries [4]. It has received considerable attention in the past few years. In order to improve the physical capabilities of soldier, the DARPA launched a project called EHPA (Exoskeleton for Human Performance Augmentation) in 2000s [6]. Funded by the DARPA, a robotic suit, Sarcos, which is aimed at “soldier of tomorrow”, is developed by the Raytheon company since 2000 [7]. Similar DARPA-funded works are underway at Massachusetts Institute of Technology (MIT) and the U.C. Berkeley. MIT designed a quasi-passive exoskeleton leg [8] and the U.C. Berkeley designed the first load-carrying lower extremity exoskeleton, referred to as BLEEX

The associate editor coordinating the review of this manuscript and approving it for publication was Youqing Wang¹.

(Berkeley Lower Extremity Exoskeleton) [9]. Almost at the same time, an exoskeleton with only one degree of freedom, called RoboKnee, is built in University of Michigan [10], and a robot suit for individuals, called HAL (Hybrid Assistive Leg) is developed in University of Tsukuba [11]. Moreover, a load cell based power assisting suit for nurse is created in Kanagawa Institute of Technology [12], and an exoskeleton driven by the wearer’s tendon is proposed to help the motion of patients and the elderly in Sogang University [13]. In addition to these, Toyota Technological Institute [14], Nanyang Technology University [15], and Technische Universität Berlin [16] also made remarkable researches on the development of exoskeleton.

Hydraulic systems are powered by high-pressure hydraulic oil. To produce the same power, an actuator system has less weight and volume than a motor, which is conducive to reducing the weight of the robot and facilitating installation [17]. Reducing power consumption is essential in a leg exoskeleton, a lower power consumption system can increase

the endurance of both the robot and the wearer. Although the exoskeleton systems that are driven by hydraulic systems have been studied in [7], [9], [18]–[20], further reducing energy cost are not well considered. As a complement, in this paper, a novel HHS that includes a unidirectional servo valve and a solenoid on-off valve is designed. Meanwhile, a novel leg exoskeleton driven by the HHS is developed and activated by using repetitive learning and on-off control based scheme.

Up to present, there have been quite a number of works that address exoskeleton control. In [21], a precise model-based sensitivity amplification control scheme is developed for the BLEEX exoskeleton without measuring any signal from the human. In [22], a human-robot coordination controller is proposed by neuromotor-based impedance control using stiffness transferred from human operator. In [23], a low-level torque sliding mode controller is presented to provide comfortable human-robot interaction. An assistive control method of a leg exoskeleton to help recovery of walking of stroke patients is described in [24]. In [25]–[27], the force control problem of exoskeleton robot is addressed. It is worth noticing that most of the actuators in the above systems are motors. In a hydraulic system, the dynamics of the actuator are with highly complexities and nonlinearities, which makes it difficult to design controller. The control input of a leg exoskeleton is always limited owing to actuator physical constraints. As one of the nonlinear constraint of control design, saturation should be specifically addressed to enhance the stability and robustness of the closed-loop system [28]. Controller design with input saturation has been widely studied in many fields, such as in industrial robot manipulators [29], underwater robot [30], nonlinear uncertain system [31], [32], and multi-input multi-output systems [33]. As we known, there are only a few papers that consider exoskeleton tracking control with input saturation [34]–[36].

During normal walking, the exoskeleton need to track the wearer's movement fittingly under a considered controller. Generally, the wearer's movement would demonstrate repetitive characteristics when they walk normally. In this regard, it is reasonable to assume the reference movement and partial dynamics maintain periodic features in theory. Repetitive learning control (RLC) is the suitable control scheme to deal with the system with periodic features [37], [38]. It is successfully used to deal with the periodic tracking tasks in [39]–[42], the unknown periodic load disturbances in [43], [44], and the non-parametric uncertainties in [45].

Aiming at decreasing power consumption of the leg exoskeleton, this paper described a novel HHS and investigated its energy saving control design. Inspired by the varieties of contact force between human leg and ground during walking, the HHS is designed to consist of a unidirectional servo valve and a solenoid on-off valve. The unidirectional servo valve is activated in the stance phase via a robust RLC with input saturation, and the solenoid valve is activated in the swing phase by on-off control scheme. The presented controller is implemented in a ARM-based embedded

microprocessor and its performance is verified on the developed leg exoskeleton by experiment.

The main contributions of the paper are summarized as follow.

- 1) A novel lower limb exoskeleton, CASWELL-II, is developed, where the mechanical structure and the embedded electronic system are integrated properly.
- 2) Aiming at reducing the energy cost in tracking control of CASWELL-II, a hybrid electro-hydraulic system that consists of unidirectional servo valve and solenoid valve is designed to drive the exoskeleton leg.
- 3) Considering the dynamics of the exoskeleton rigid body and its constrained actuators, a full model of exoskeleton driven by hybrid electro-hydraulic actuators with input saturation is achieved.
- 4) A robust RLC scheme is designed and implemented in the embedded electronic system for the tracking control of CASWELL-II. The efficacy of the leaning-based controller has been verified by the experimental result. In addition, the power consumption of the proposed system is almost 30% less than that of systems with bidirectional electro-hydraulic actuators.

The rest of this paper is organized as follows. The development of leg exoskeleton, which includes the HHS, the mechanical structure, and embedded electronic system, are all addressed in Section II. Then, the full dynamics of system is modelled in Section III. Consequently, under the framework of backstepping design and Lyapunov theory, the robust RLC design and stability analysis are considered rigorously in Section IV. Experiments are carried out to illustrate the effectiveness of the whole exoskeleton system in Section V. The conclusion and future work are drawn in Section VI.

II. DESIGN OF LEG EXOSKELETON

A. HHS

As shown in Fig. 1, human's normal walking cycle can be divided into two sub-phases: the stance phase and the swing phase. It is clear that the human leg only bears body weight in the stance phase. Moreover, in the swing phase of a walking cycle, the exoskeleton leg only needs to follow the movement of the human leg without bearing weight. This fact motivates us to drive the exoskeleton only in the stance phase during the normal walking process. In such a way, compared with the fully-driven situation, high-pressure hydraulic oil is needed only in the stance phase, which leads to considerable power reduction.

The schematic of the HHS which includes a unidirectional servo valve and a solenoid on-off valve is shown in Fig. 2(b). Its working process is described as follows. In the stance phases of a walking cycle, the solenoid on-off valve is closed, and meanwhile the exoskeleton is driven by the unidirectional hydraulic actuator to track the movement of human. In the swing phase, the servo valve is turned into the closed state, and the solenoid on-off valve is opened simultaneously to release the pressure of hydraulic cylinder rapidly so that the exoskeleton is bent by the human leg.

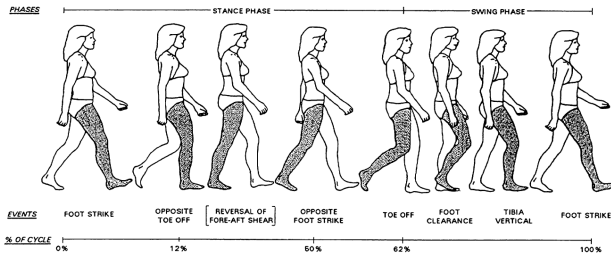


FIGURE 1. The human walking cycle.

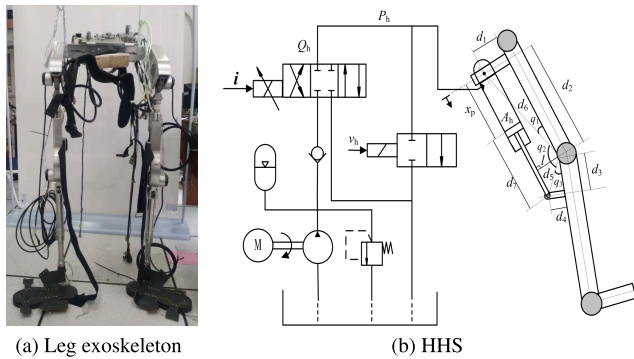


FIGURE 2. The leg exoskeleton and the HHS.

B. MECHANICAL STRUCTURE

The mechanical structure of the leg exoskeleton is shown in Fig. 2(a), where the HHS is integrated into the back of exoskeleton body. A build-in space is designed in the back-side of the exoskeleton to install the lithium battery (Voltage: 24V, Capacity: 40Ah), which provides the power source of the whole exoskeleton system. Each leg of the exoskeleton has five degree of freedoms (DOF), namely the hip flexion/extension (1 DOF), the knee flexion/extension (1 DOF), and the ankle plantar flexion/dorsiflexion (3 DOFs), where the first two items are driven by the HHS. The hydraulic actuators of the hip joint and the knee joint are installed in the horizontal direction and the vertical direction, respectively. Elastic bandages and plastic shoes are designed to tie the exoskeleton and the wearer together at the relevant junctions.

C. EMBEDDED ELECTRONIC SYSTEM

As the information processing and control center of the exoskeleton for human power augmentation, the embedded electronic system is crucial. It is responsible for collecting sensor data, implementing the controller, and driving the HHS. The embedded electronic system of the leg exoskeleton is shown in Fig. 3, which includes the input channels for collecting sensor data, analog to digital converter (ADC) for digitizing input signals, microprocessor for information processing and control, digital to analog converter (DAC), and output channels for driving the HHS.

III. MODELLING AND PROBLEM FORMULATION

The mathematical model of the leg exoskeleton contains the rigid body part and the HHS part. By using the Lagrangian

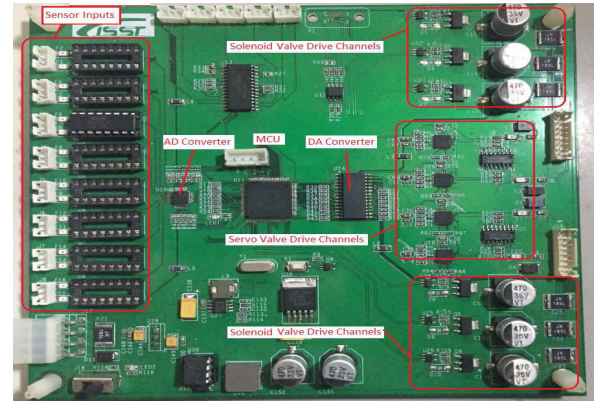


FIGURE 3. The embedded electronic system.

dynamics method, the rigid body model of the leg exoskeleton can be simplified as follows [47],

$$M(q)\ddot{q} + C(q, \dot{q})\dot{q} + G(q) = \tau + d(t), \quad (1)$$

where q, \dot{q} , and $\ddot{q} \in \mathcal{R}^n$ denote the joints angles, joints angular velocities, and joints angular accelerations, respectively. $M(q) \in \mathcal{R}^{n \times n}$, $C(q, \dot{q}) \in \mathcal{R}^{n \times n}$, and $G(q) \in \mathcal{R}^n$ are the inertia matrix, the centrifugal matrix, and the gravitational force vector, respectively. $\tau \in \mathcal{R}^n$ denotes the joint torque of the HHS and $d(t) \in \mathcal{R}^n$ denotes the unknown disturbances between the leg exoskeleton and wearer. When the periodic movement is dominant in wearer's normal walking, we can consider the unknown disturbances $d(t)$ to be periodic, where the period is equal to that of wearer's walking gait [46]. For system (1), the following properties are valid [47].

Property 1: The matrix $M(q)$ is symmetric and positive definite.

Property 2: The matrix $\dot{M}(q) - 2C(q, \dot{q})$ is skew symmetric.

Since the torque acting on the exoskeleton joint is provided by the HHS, the dynamics of the HHS are considered simultaneously. The torque can be described as follows according to Newton mechanics principle

$$\tau = (A_h P_h + f_c)l, \quad (2)$$

where A_h is the piston area of the hydraulic cylinder, and f_c is the equivalent force acted on the piston rod. In addition, P_h is the intensity of pressure in the hydraulic cylinder, satisfying the following dynamics [48],

$$\dot{P}_h = \frac{\beta_e}{V_0 + A_h x_p} (Q_h - A_h \dot{x}_p), \quad (3)$$

where β_e is a constant bulk modulus of the high-pressure hydraulic oil, Q_h denotes the flow rate of the unidirectional servo valve, V_0 denotes the initial volume of the chamber of the hydraulic cylinder, and x_p denotes the displacement of the piston rod of the HHS which can be described via the following trigonometric

$$x_p = \sqrt{d_5^2 + d_6^2 - 2d_5d_6 \cos q_2} - d_7 \quad (4)$$

where d_5 , d_6 and d_7 are constants related to mechanical structures, q_2 is uniquely determined by q

$$q_2 = q - q_1 - q_3, \quad (5)$$

with constants $q_1 = \arctan(d_1/d_2)$ and $q_3 = \arctan(d_4/d_3)$. From (4) and (5), we can conclude that x_p corresponds to the joint angle q one by one. l is the arm of force provided by the HHS, which can be obtained using the equal area principle of triangle

$$d_5 d_6 \sin q_2 = l(x_p + d_7). \quad (6)$$

In essence, the frequency of human normal walking is much less than that of valves. Thus, the flow rate of the unidirectional valve Q_h in (3) is related to its current i proportionally [49]

$$Q_h = \begin{cases} Ki, & \dot{x}_p \geq 0, \\ 0, & \dot{x}_p < 0, \end{cases} \quad (7)$$

where K is a constant gain.

The amplitude of the input current i of the unidirectional servo valve is limited owing to its physical constraint in single direction, and can be expressed asymmetrically

$$i = S(u) = \begin{cases} I_{max}, & u \geq I_{max}, \\ u, & 0 < u < I_{max}, \\ 0, & u \leq 0, \end{cases} \quad (8)$$

where i and I_{max} are the valid and maximum currents of the unidirectional valve, and u is the actual controller that will be designed. The difference between the valid input current i of the servo valve and the actual input u of the controller, denoted by Δ , can be written as

$$\Delta \triangleq i - v = S(u) - u. \quad (9)$$

Remark 1: Owing to the repetitiveness of the wearer's normal walking, it is rational to assume that both the equivalent force f_c in (2) and the difference Δ in (9) possess certain repetitive characteristics. Meanwhile, non-repetitive disturbance or noise that would have an upper bound also might be involved into f_c and Δ . As a consequence, both the equivalent force f_c and the control difference Δ can be regarded as a combination of periodic components (denoted by f_p and Δ_p) and non-periodic components (denoted by f_n and Δ_n), which can be described in the following

$$\begin{cases} f_c = f_p + f_n, & \Delta = \Delta_p + \Delta_n, \\ f_p(t) = f_p(t - N), & \Delta_p(t) = \Delta_p(t - N), \\ f_n \leq \bar{f}_n, & \Delta_n \leq \bar{\Delta}_n. \end{cases} \quad (10)$$

where $N > 0$ is the constant period.

Now, combining the dynamics of the rigid body and the HHS, the dynamics of the whole system are considered. Let $\mathbf{q} \triangleq [q_j]^T$, $\boldsymbol{\tau} \triangleq [\tau_j]^T$, $\mathbf{l} \triangleq \text{diag}[l_j]$, $\mathbf{P}_h \triangleq [P_j]^T$, $\mathbf{f}_c \triangleq [f_{cj}]^T$, $\mathbf{A}_h \triangleq \text{diag}[A_{hj}]$, $\mathbf{x}_p \triangleq [x_{pj}]^T$, and $\mathbf{u} = [u_j]^T$, where the subscript $j = 1, \dots, 4$ represent the four actuated joints, i.e., the hip and knee joints of the left and right leg.

Let $\mathbf{x}_1 = \mathbf{q}$, $\mathbf{x}_2 = \dot{\mathbf{q}}$, $\mathbf{x}_3 = \mathbf{A}_h \mathbf{P}_h$. By combining the rigid body dynamic in (1) and the HHS dynamics in (2), (3), (7), and (9), the state space model of the leg exoskeleton driven by the HHS is

$$\begin{cases} \dot{\mathbf{x}}_1 = \mathbf{x}_2, \\ \dot{\mathbf{x}}_2 = \mathbf{M}(\mathbf{x}_1)^{-1} [\mathbf{I}(\mathbf{x}_3 + \mathbf{f}_p + \mathbf{f}_n) + \mathbf{d}(t) \\ \quad - \mathbf{C}(\mathbf{x}_1, \dot{\mathbf{x}}_1) \mathbf{x}_2 - \mathbf{G}(\mathbf{x}_1)], \\ \dot{\mathbf{x}}_3 = -\mathbf{g}_1(\mathbf{x}_p) \dot{\mathbf{x}}_p + \mathbf{g}_2(\mathbf{x}_p) \Delta_p + \mathbf{g}_2(\mathbf{x}_p) \Delta_n \\ \quad + \mathbf{g}_2(\mathbf{x}_p) \mathbf{u}. \end{cases} \quad (11)$$

where

$$\begin{aligned} \mathbf{g}_m(\mathbf{x}_p) &= \text{diag}[g_m(x_{pj})], \quad m = 1, 2, j = 1, \dots, 4, \\ g_1(x_{pj}) &= \frac{A_{hj}^2 \beta_e}{V_{0j} + A_{hj} x_{pj}}, \quad g_2(x_{pj}) = \frac{A_{hj} \beta_e K}{V_{0j} + A_{hj} x_{pj}} \end{aligned} \quad (12)$$

The control objective of the leg exoskeleton is to design an actual control input u for the HHS, such that the output movement of the leg exoskeleton $\mathbf{y} = \mathbf{x}_1$ can track the wearer's movement \mathbf{q}_r closely. It is clear that, when walking normally, the motion of human would demonstrate repetitive characteristics in general. Hence, without loss of generality, it is assumed that the movement of the wearer, \mathbf{q}_r , is periodic, satisfying

$$\mathbf{q}_r(t) = \mathbf{q}_r(t - N). \quad (13)$$

where $N > 0$ is the period. When \mathbf{q}_r is differentiable, its first and second derivatives are also periodic.

IV. CONTROLLER DESIGN AND MAIN RESULTS

The energy saving control of the leg exoskeleton will be addressed in this section. As the exoskeleton leg is bent by the human leg passively in the swing phase, the controller design is investigated only in the stance phase. A robust RLC is carried out by utilizing the backstepping technique, and the convergence of the system in the stance phase is analyzed using the Lyapunov method. Before proceeding to the controller design, the following *Lemma* is given by expanding *Property 2* of [50] from scalar case to vector case to facilitate the controller design.

Lemma 1: Let $H(t)$, $\hat{H}(t)$, $\tilde{H}(t)$, and $s(t) \in \mathcal{R}^n$, if the following relationships hold

$$\begin{aligned} H(t) &= H(t - N), \\ \tilde{H}(t) &= H(t) - \hat{H}(t), \\ \hat{H}(t) &= \hat{H}(t - N) + s(t). \end{aligned} \quad (14)$$

The upper right-hand derivative of $\int_{t-N}^t \tilde{H}^T(\mu) \tilde{H}(\mu) d\mu$ is

$$-2\tilde{H}^T(t)s(t) - s^T(t)s(t).$$

A. CONTROLLER DESIGN

Step 1. Define the errors

$$\mathbf{e}_1 = \mathbf{x}_1 - \mathbf{x}_{1d}, \quad \mathbf{e}_2 = \mathbf{x}_2 - \mathbf{a}_1, \quad \mathbf{e}_3 = \mathbf{x}_3 - \mathbf{a}_2, \quad (15)$$

where $\mathbf{x}_{1d} \triangleq \mathbf{q}_d$ is the desired movement of the leg exoskeleton, and $\mathbf{a}_1, \mathbf{a}_2$ are intermediate control inputs used to stabilize the system. The time derivative of \mathbf{e}_1 is

$$\dot{\mathbf{e}}_1 = \mathbf{x}_2 - \dot{\mathbf{x}}_{1d} = \mathbf{e}_2 + \mathbf{a}_1 - \dot{\mathbf{x}}_{1d}. \quad (16)$$

If we design

$$\mathbf{a}_1 = -k_1 \mathbf{e}_1 + \dot{\mathbf{x}}_{1d}, \quad k_1 > 0, \quad (17)$$

then combining the above two equations renders to

$$\dot{\mathbf{e}}_1 = -k_1 \mathbf{e}_1 + \mathbf{e}_2. \quad (18)$$

Step 2. By substituting (11), the time derivative of \mathbf{e}_2 is

$$\begin{aligned} \dot{\mathbf{e}}_2 &= \dot{\mathbf{x}}_2 - \dot{\mathbf{a}}_1 \\ &= M(\mathbf{x}_1)^{-1} [\mathbf{l}(\mathbf{x}_3 + \mathbf{f}_p + \mathbf{f}_n) + \mathbf{d}(t) \\ &\quad - C(\mathbf{x}_1, \dot{\mathbf{x}}_1) \mathbf{x}_2 - G(\mathbf{x}_1)] - \dot{\mathbf{a}}_1 \\ &= M(\mathbf{x}_1)^{-1} [\mathbf{l}(\mathbf{e}_3 + \mathbf{a}_2 + \mathbf{f}_p + \mathbf{f}_n) + \mathbf{d}(t) \\ &\quad - C(\mathbf{x}_1, \dot{\mathbf{x}}_1) \mathbf{x}_2 - G(\mathbf{x}_1)] - \dot{\mathbf{a}}_1. \end{aligned}$$

Further design \mathbf{a}_2 as

$$\mathbf{a}_2 = \mathbf{a}_{2a} + \mathbf{a}_{2b} + \mathbf{a}_{2c}, \quad (19)$$

where

(i) \mathbf{a}_{2a} is the feedback control part,

$$\mathbf{a}_{2a} = \mathbf{l}^{-1} [-k_2 \mathbf{e}_2 - k_f \mathbf{f}_n - \mathbf{e}_1], \quad (20)$$

k_2 and k_f are positive gains, and \mathbf{l} is defined in (6).

(ii) \mathbf{a}_{2b} is the learning control part,

$$\mathbf{a}_{2b} = -\mathbf{l}^{-1} \hat{\mathbf{p}}_1(t), \quad (21)$$

where

$$\hat{\mathbf{p}}_1(t) = \begin{cases} \hat{\mathbf{p}}_1(t - N) + k_3 \mathbf{e}_2, & k_3 > 0, \quad t > N \\ \mathbf{0}, & t \in [0, N]. \end{cases} \quad (22)$$

(iii) \mathbf{a}_{2c} is the robust stabilization part,

$$\mathbf{a}_{2c} = -\mathbf{l}^{-1} k_4 \mu^2(\|\xi\|) \mathbf{e}_2, \quad (23)$$

where ξ is given as

$$\xi = [e_1^T, \dot{e}_1^T]^T, \quad (24)$$

$k_4 > 0$ is a constant gain, and $\mu(\cdot)$ is a positive bounding function.

Step 3. Differentiating \mathbf{e}_3 yields

$$\dot{\mathbf{e}}_3 = -\mathbf{g}_1(\mathbf{x}_p) \dot{\mathbf{x}}_p + \mathbf{g}_2(\mathbf{x}_p) \Delta_p + \mathbf{g}_2(\mathbf{x}_p) \Delta_n + \mathbf{g}_2(\mathbf{x}_p) v - \dot{\mathbf{a}}_2. \quad (25)$$

The controller is designed as

$$\mathbf{u} = \mathbf{g}_2(\mathbf{x}_p)^{-1} [-\mathbf{l} \mathbf{e}_2 + \mathbf{g}_1(\mathbf{x}_p) \dot{\mathbf{x}}_p - \mathbf{g}_2(\mathbf{x}_p) \hat{\mathbf{p}}_2(t) - k_\Delta \mathbf{g}_2(\mathbf{x}_p) \bar{\Delta}_n + \dot{\mathbf{a}}_2], \quad (26)$$

where

$$\hat{\mathbf{p}}_2(t) = \begin{cases} \hat{\mathbf{p}}_2(t - N) + k_5 \mathbf{e}_3, & k_5 > 0, \quad t > N \\ \mathbf{0}, & t \in [0, N]. \end{cases} \quad (27)$$

In (26), $\hat{\mathbf{p}}_2(t)$ is used to deal with the periodic difference $\mathbf{p}_2(t) = \Delta_p$ in (10).

Now, it follows from (25) and (26) that

$$\dot{\mathbf{e}}_3 = \tilde{\mathbf{p}}_2(t) + \mathbf{g}_2(\mathbf{x}_p) \Delta_n - k_\Delta \mathbf{g}_2(\mathbf{x}_p) \bar{\Delta}_n(v) - \mathbf{l} \mathbf{e}_2. \quad (28)$$

B. MAIN RESULTS

Theorem 1: Consider the leg exoskeleton driven by the HHS in (11), under *Assumption* (13), with the robust RLC (26). When the design parameters $k_i, i = 1, \dots, 5, k_f, k_\Delta$ satisfy

$$\begin{cases} k_2 + \frac{1}{2k_3} - \frac{1}{4k_4} > 0, \\ [1ex] k_f > \|\mathbf{l}\|, \quad k_\Delta > 1, \end{cases} \quad (29)$$

all the signals of the closed-loop system are bounded and the tracking error of the leg exoskeleton in the stance phase will converge to zero asymptotically.

Proof: Consider the following Lyapunov functional candidate

$$\begin{aligned} V(t) &= V_1(t) + V_2(t), \\ V_1(t) &= \frac{1}{2} \mathbf{e}_1^T \mathbf{e}_1 + \frac{1}{2} \mathbf{e}_2^T M(\mathbf{x}_1) \mathbf{e}_2 + \frac{1}{2} \mathbf{e}_3^T \mathbf{e}_3, \\ V_2(t) &= \frac{1}{2k_3} \int_{t-N}^t \tilde{\mathbf{p}}_1^T(\varsigma_1) \tilde{\mathbf{p}}_1(\varsigma_1) d\varsigma_1 \\ &\quad + \frac{1}{2k_5} \int_{t-N}^t \tilde{\mathbf{p}}_2^T(\varsigma_2) \tilde{\mathbf{p}}_2(\varsigma_2) d\varsigma_2, \end{aligned} \quad (30)$$

where $\tilde{\mathbf{p}}_i(t) \triangleq \mathbf{p}_i(t) - \hat{\mathbf{p}}_i(t), i = 1, 2$.

First, differentiating $V_1(t)$ with respect to time, we obtain

$$\dot{V}_1(t) = \mathbf{e}_1^T \dot{\mathbf{e}}_1 + \mathbf{e}_2^T M(\mathbf{x}_1) \dot{\mathbf{e}}_2 + \frac{1}{2} \mathbf{e}_2^T \dot{M}(\mathbf{x}_1) \mathbf{e}_2 + \mathbf{e}_3^T \dot{\mathbf{e}}_3. \quad (31)$$

Then, considering (18), (19), and (28), it follows that

$$\begin{aligned} \dot{V}_1(t) &= \mathbf{e}_1^T (-k_1 \mathbf{e}_1 + \mathbf{e}_2) + \mathbf{e}_2^T M(\mathbf{x}_1) \dot{\mathbf{e}}_2 \\ &\quad + \frac{1}{2} \mathbf{e}_2^T \dot{M}(\mathbf{x}_1) \mathbf{e}_2 + \mathbf{e}_3^T \dot{\mathbf{e}}_3 \\ &= -k_1 \mathbf{e}_1^T \mathbf{e}_1 + \mathbf{e}_1^T \mathbf{e}_2 + \frac{1}{2} \mathbf{e}_2^T \dot{M}(\mathbf{x}_1) \mathbf{e}_2 + \mathbf{e}_3^T \dot{\mathbf{e}}_3 \\ &\quad + \mathbf{e}_2^T M(\mathbf{x}_1) [M(\mathbf{x}_1)^{-1} [\mathbf{l}(\mathbf{e}_3 + \mathbf{a}_2 + \mathbf{f}_p + \mathbf{f}_n) \\ &\quad + \mathbf{d}(t) - C(\mathbf{x}_1, \dot{\mathbf{x}}_1) \mathbf{x}_2 - G(\mathbf{x}_1)] - \dot{\mathbf{a}}_1] \\ &= -k_1 \mathbf{e}_1^T \mathbf{e}_1 + \mathbf{e}_1^T \mathbf{e}_2 + \frac{1}{2} \mathbf{e}_2^T \dot{M}(\mathbf{x}_1) \mathbf{e}_2 + \mathbf{e}_3^T \dot{\mathbf{e}}_3 \\ &\quad + \mathbf{e}_2^T [\mathbf{l}(\mathbf{e}_3 + \mathbf{a}_2 + \mathbf{f}_p + \mathbf{f}_n) + \mathbf{d}(t) \\ &\quad - C(\mathbf{x}_1, \dot{\mathbf{x}}_1) (\mathbf{e}_2 + \mathbf{a}_1) - G(\mathbf{x}_1) - M(\mathbf{x}_1) \dot{\mathbf{a}}_1]. \end{aligned}$$

Now, substituting (17) into (32) and applying *Property 2*,

$$\begin{aligned} \dot{V}_1(t) &= -k_1 \mathbf{e}_1^T \mathbf{e}_1 + \mathbf{e}_1^T \mathbf{e}_2 + \mathbf{e}_3^T \dot{\mathbf{e}}_3 \\ &\quad + \mathbf{e}_2^T [\mathbf{l}(\mathbf{e}_3 + \mathbf{a}_2 + \mathbf{f}_p + \mathbf{f}_n) + \mathbf{d}(t) \\ &\quad - C(\mathbf{x}_1, \dot{\mathbf{x}}_1) \mathbf{a}_1 - G(\mathbf{x}_1) - M(\mathbf{x}_1) \dot{\mathbf{a}}_1] \\ &= -k_1 \mathbf{e}_1^T \mathbf{e}_1 + \mathbf{e}_1^T \mathbf{e}_2 + \mathbf{e}_3^T \dot{\mathbf{e}}_3 \\ &\quad + \mathbf{e}_2^T [\mathbf{l}(\mathbf{e}_3 + \mathbf{a}_2 + \mathbf{f}_p + \mathbf{f}_n) + \mathbf{d}(t) \\ &\quad - C(\mathbf{x}_1, \dot{\mathbf{x}}_1) (-k_1 \mathbf{e}_1 + \dot{\mathbf{x}}_{1d}) - G(\mathbf{x}_1) \end{aligned}$$

$$\begin{aligned}
 & -M(\mathbf{x}_1)(-k_1\dot{\mathbf{e}}_1 + \ddot{\mathbf{x}}_{1d}) \\
 = & -k_1\mathbf{e}_1^T\mathbf{e}_1 + \mathbf{e}_1^T\mathbf{e}_2 + \mathbf{e}_3^T\dot{\mathbf{e}}_3 \\
 & + \mathbf{e}_2^T[\mathbf{l}(\mathbf{e}_3 + \mathbf{a}_2 + \mathbf{f}_p + \mathbf{f}_n) + \mathbf{d}(t) \\
 & - G(\mathbf{x}_1) - C(\mathbf{x}_1, \dot{\mathbf{x}}_1)\dot{\mathbf{x}}_{1d} - M(\mathbf{x}_1)\ddot{\mathbf{x}}_{1d} \\
 & + k_1C(\mathbf{x}_1, \dot{\mathbf{x}}_1)\dot{\mathbf{e}}_1 + k_1M(\mathbf{x}_1)\dot{\mathbf{e}}_1] \quad (32)
 \end{aligned}$$

Define

$$\begin{aligned}
 \boldsymbol{\eta} & \triangleq -M(\mathbf{x}_{1d})\ddot{\mathbf{x}}_{1d} - C(\mathbf{x}_{1d}, \dot{\mathbf{x}}_{1d})\dot{\mathbf{x}}_{1d} - G(\mathbf{x}_{1d}), \\
 \boldsymbol{\zeta} & \triangleq -M(\mathbf{x}_1)(\ddot{\mathbf{x}}_{1d} - k_1\dot{\mathbf{e}}_1) - C(\mathbf{x}_1, \dot{\mathbf{x}}_1)(\dot{\mathbf{x}}_{1d} - k_1\mathbf{e}_1) \\
 & - G(\mathbf{x}_1) - \boldsymbol{\eta}. \quad (33)
 \end{aligned}$$

Then, by substituting (33) into (32), we have

$$\begin{aligned}
 \dot{V}_1(t) = & -k_1\mathbf{e}_1^T\mathbf{e}_1 + \mathbf{e}_1^T\mathbf{e}_2 + \mathbf{e}_3^T\dot{\mathbf{e}}_3 + \mathbf{e}_2^T[\mathbf{l}(\mathbf{e}_3 + \mathbf{a}_2) \\
 & + \mathbf{l}\mathbf{f}_n + \mathbf{l}\mathbf{f}_p + \mathbf{d}(t) + \boldsymbol{\zeta} + \boldsymbol{\eta}], \quad (34)
 \end{aligned}$$

where the unknown disturbances $\mathbf{d}(t)$ and the partial equivalent force \mathbf{f}_p are assumed to be periodic, and $\boldsymbol{\eta}$ is also periodic due to the desired movement \mathbf{x}_{1d} . Let $\mathbf{p}_1(t) \triangleq \mathbf{l}\mathbf{f}_p + \mathbf{d}(t) + \boldsymbol{\eta}$, implying that

$$\mathbf{p}_1(t) = \mathbf{p}_1(t - N). \quad (35)$$

Further substituting (35) into (34), we can see that

$$\begin{aligned}
 \dot{V}_1(t) = & -k_1\mathbf{e}_1^T\mathbf{e}_1 + \mathbf{e}_1^T\mathbf{e}_2 + \mathbf{e}_3^T\dot{\mathbf{e}}_3 \\
 & + \mathbf{e}_2^T[\mathbf{l}(\mathbf{e}_3 + \mathbf{a}_2) + \mathbf{l}\mathbf{f}_n + \mathbf{p}_1(t) + \boldsymbol{\zeta}] \quad (36)
 \end{aligned}$$

where $\boldsymbol{\zeta}$ satisfies the following inequality proved in [41]

$$\|\boldsymbol{\zeta}\| \leq \mu(\|\boldsymbol{\xi}\|)\|\boldsymbol{\xi}\|. \quad (37)$$

Considering (19), (28), and (36), we can get

$$\begin{aligned}
 \dot{V}_1(t) = & -k_1\mathbf{e}_1^T\mathbf{e}_1 - k_2\mathbf{e}_2^T\mathbf{e}_2 + \mathbf{e}_2^T\tilde{\mathbf{p}}_1(t) + \mathbf{e}_3^T\tilde{\mathbf{p}}_2(t) \\
 & + \mathbf{e}_2^T\boldsymbol{\zeta} - \mathbf{e}_2^T k_4\mu^2(\|\boldsymbol{\xi}\|)\mathbf{e}_2 + \mathbf{e}_2^T(-k_f\bar{\mathbf{f}}_n + \mathbf{l}\mathbf{f}_n) \\
 & + \mathbf{e}_3^T(\mathbf{g}_2(\mathbf{x}_p)\Delta_n - k_\Delta\mathbf{g}_2(\mathbf{x}_p)\bar{\Delta}_n) \quad (38)
 \end{aligned}$$

Second, the time derivative of $V_2(t)$ is

$$\begin{aligned}
 \dot{V}_2(t) = & \frac{1}{2k_3}[\tilde{\mathbf{p}}_1^T(t)\tilde{\mathbf{p}}_1(t) - \tilde{\mathbf{p}}_1^T(t - N)\tilde{\mathbf{p}}_1(t - N)] \\
 & + \frac{1}{2k_5}[\tilde{\mathbf{p}}_2^T(t)\tilde{\mathbf{p}}_2(t) - \tilde{\mathbf{p}}_2^T(t - N)\tilde{\mathbf{p}}_2(t - N)]. \quad (39)
 \end{aligned}$$

By Lemma 1, (22), (27), and (35), we can see that

$$\begin{aligned}
 \dot{V}_2(t) = & \frac{1}{2k_3}[-2k_3\tilde{\mathbf{p}}_1^T(t)\mathbf{e}_2 - k_3^2\mathbf{e}_2^T\mathbf{e}_2] \\
 & + \frac{1}{2k_5}[-2k_5\tilde{\mathbf{p}}_2^T(t)\mathbf{e}_3 - k_5^2\mathbf{e}_3^T\mathbf{e}_3] \\
 = & -\tilde{\mathbf{p}}_1^T(t)\mathbf{e}_2 - \frac{1}{2}k_3\mathbf{e}_2^T\mathbf{e}_2 \\
 & -\tilde{\mathbf{p}}_2^T(t)\mathbf{e}_3 - \frac{1}{2}k_5\mathbf{e}_3^T\mathbf{e}_3 \quad (40)
 \end{aligned}$$

Third, combining (38) and (40) gives

$$\begin{aligned}
 \dot{V}(t) = & -k_1\mathbf{e}_1^T\mathbf{e}_1 - k_2\mathbf{e}_2^T\mathbf{e}_2 + \mathbf{e}_2^T\tilde{\mathbf{p}}_1(t) + \mathbf{e}_3^T\tilde{\mathbf{p}}_2(t) \\
 & + \mathbf{e}_2^T\boldsymbol{\zeta} - \mathbf{e}_2^T k_4\mu^2(\|\boldsymbol{\xi}\|)\mathbf{e}_2
 \end{aligned}$$

$$\begin{aligned}
 & + \mathbf{e}_2^T(-k_f\bar{\mathbf{f}}_n + \mathbf{l}\mathbf{f}_n) - \tilde{\mathbf{p}}_2^T(t)\mathbf{e}_3 - \frac{1}{2}k_5\mathbf{e}_3^T\mathbf{e}_3 \\
 & + \mathbf{e}_3^T(\mathbf{g}_2(\mathbf{x}_p)\Delta_n - k_\Delta\mathbf{g}_2(\mathbf{x}_p)\bar{\Delta}_n) \\
 & - \tilde{\mathbf{p}}_1^T(t)\mathbf{e}_2 - \frac{1}{2}k_3\mathbf{e}_2^T\mathbf{e}_2 \\
 = & -k_1\mathbf{e}_1^T\mathbf{e}_1 - k_2\mathbf{e}_2^T\mathbf{e}_2 - \frac{1}{2}k_3\mathbf{e}_2^T\mathbf{e}_2 - \frac{1}{2}k_5\mathbf{e}_3^T\mathbf{e}_3 \\
 & + \mathbf{e}_2^T\boldsymbol{\zeta} - \mathbf{e}_2^T k_4\mu^2(\|\boldsymbol{\xi}\|)\mathbf{e}_2 \\
 & + \mathbf{e}_2^T(\mathbf{l}\mathbf{f}_n - k_f\bar{\mathbf{f}}_n) \\
 & + \mathbf{e}_3^T(\mathbf{g}_2(\mathbf{x}_p)\Delta_n - k_\Delta\mathbf{g}_2(\mathbf{x}_p)\bar{\Delta}_n) \\
 \leq & -k_1\mathbf{e}_1^T\mathbf{e}_1 - k_2\mathbf{e}_2^T\mathbf{e}_2 - \frac{1}{2}k_3\mathbf{e}_2^T\mathbf{e}_2 - \frac{1}{2}k_5\mathbf{e}_3^T\mathbf{e}_3 \\
 & + \mu(\|\boldsymbol{\xi}\|)\|\boldsymbol{\xi}\|\|\mathbf{e}_2\| - k_4\mu^2(\|\boldsymbol{\xi}\|)\|\mathbf{e}_2\|^2 \\
 & + \|\mathbf{e}_2\|(\|\mathbf{l}\|\|\bar{\mathbf{f}}_n\| - k_f\|\bar{\mathbf{f}}_n\|) \quad (41) \\
 & + \|\mathbf{e}_3\|(\|\mathbf{g}_2(\mathbf{x}_p)\|\|\bar{\Delta}_n\| - k_\Delta\|\mathbf{g}_2(\mathbf{x}_p)\|\|\bar{\Delta}_n\|).
 \end{aligned}$$

Considering the definition of $\boldsymbol{\xi}$ in (24), it follows that

$$\mu(\|\boldsymbol{\xi}\|)\|\boldsymbol{\xi}\|\|\mathbf{e}_2\| - k_4\mu^2(\|\boldsymbol{\xi}\|)\|\mathbf{e}_2\|^2 \leq \frac{1}{4k_4}\|\mathbf{e}_2\|^2. \quad (42)$$

Substituting (42) into (41) renders to

$$\begin{aligned}
 \dot{V}(t) \leq & -k_1\mathbf{e}_1^T\mathbf{e}_1 - k_2\mathbf{e}_2^T\mathbf{e}_2 - \frac{1}{2}k_3\mathbf{e}_2^T\mathbf{e}_2 - \frac{1}{2}k_5\mathbf{e}_3^T\mathbf{e}_3 \\
 & + \frac{1}{4k_4}\|\mathbf{e}_2\|^2 + \|\mathbf{e}_2\|\|\bar{\mathbf{f}}_n\|(\|\mathbf{l}\| - k_f) \\
 & + \|\mathbf{e}_3\|\|\mathbf{g}_2(\mathbf{x}_p)\|\|\bar{\Delta}_n\|(1 - k_\Delta) \\
 \leq & -k_1\mathbf{e}_1^T\mathbf{e}_1 - (k_2 + \frac{1}{2}k_3 - \frac{1}{4k_4})\mathbf{e}_2^T\mathbf{e}_2 - \frac{1}{2}k_5\mathbf{e}_3^T\mathbf{e}_3 \\
 & + \|\mathbf{e}_2\|\|\bar{\mathbf{f}}_n\|(\|\mathbf{l}\| - k_f) \\
 & + \|\mathbf{e}_3\|\|\mathbf{g}_2(\mathbf{x}_p)\|\|\bar{\Delta}_n\|(1 - k_\Delta). \quad (43)
 \end{aligned}$$

Using the parametric constraints in (29), it is concluded that $\dot{V}(t) \leq 0$. By adopting the Barbalat's Lemma [51], \mathbf{e}_1 will converge to zero asymptotically.

Now, the remaining work is to analyze the boundedness of all signals involved in the control process of leg exoskeleton. From (43), $V(t)$ is nonincreasing in the time domain, implying that $\mathbf{e}_i, i = 1, 2, 3$ and $\mathbf{p}_i, i = 1, 2$ are bounded. Noticing the boundedness of the control input that is ensured by (8), and the passivity property of the exoskeleton system, the boundedness of the states, $\mathbf{x}_i, i = 1, \dots, 3$, is guaranteed.

V. EXPERIMENTAL RESULTS

In order to verify the control performance of the leg exoskeleton driven by the HHS, the energy saving control scheme that includes the robust RLC in the stance phase and on-off control in the swing phase is implemented and verified. The setup of the experimental apparatus is first introduced. Then the parametric setting and controller implementation are given. At last, the experimental results are demonstrated with further discussion.

A. EXPERIMENT SETUP

The schematic of the experimental structure is shown in Fig. 4. Note that the exoskeleton leg is driven by the

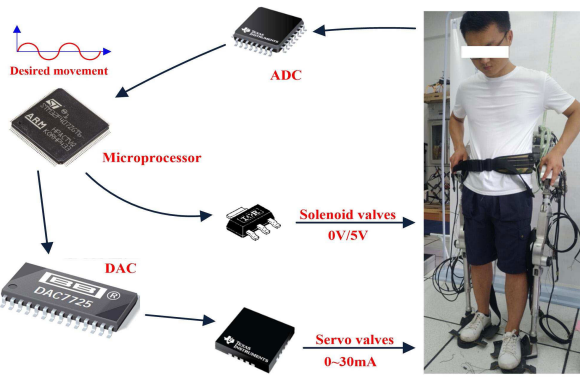


FIGURE 4. Control structure of the leg exoskeleton.

unidirectional servo valve only in the stance phase during a walking cycle. Thus, the flexion movement is performed by the experimenter to simulate the movement of human leg in the swing phase.

As mentioned before, the leg exoskeleton is a high-density robot for human power augmentation. The exoskeleton rigid body, the HHS which includes the unidirectional servo valves and the solenoid on-off valve, and the hydraulic pump are all integrated. A 24V/40Ah lithium battery is used to supply the exoskeleton system, including the hydraulic pump and the embedded electronic system. The chip used in the embedded electronic system is a ARM based 32-bit microprocessor, called STM32F407, which is the only chip used to implement the controller and work at the frequency of 100MHz in the experiment. A 8 input channels ADC chip, called ADS7852Y, is used to sample the sensor data. A 4 output channels DAC chip, called DAC7725U, is adopted to generate the driven current of the unidirectional servo valves by incorporating the current converter chip XTR300AIRGW. The N-channel MOSFET IRFL014 and its driver chip UCC27517 are designed to control the solenoid on-off valves of the HHS.

B. CONTROLLER IMPLEMENTATION AND PARAMETERS

The proposed control scheme is implemented in the microprocessor using C language, which is the most widely used language in the industrial and engineering applications. The controller is divided into two parts during a walking cycle: (1) in the stance phase, the exoskeleton leg is driven by unidirectional servo valve via the proposed robust RLC, and (2) in the swing phase, the exoskeleton is driven by the human leg by opening the solenoid valve.

In order to facilitate the calculation in the control process, the periodic reference trajectory is given as a sinusoidal curve and generated in the microprocessor via an array of 128 elements. The parameters of the HHS are $\beta_e = 1.2 \times 10^9 N/m^2$, $A_h = 6 \times 10^{-4} m^2$, $V_0 = 80 \times 10^{-6} m^3$, $K = 0.95$. The current saturations of the servo valves are chosen as 30 mA. Further, the control parameters are set as $k_1 = 28$, $k_2 = 35$, $k_3 = 17$, $k_4 = 30$, $k_5 = 20$, $k_f = 30$, $k_\Delta = 12$, $\mu = 45$, which meet all the requirements in *Theorem 1*.

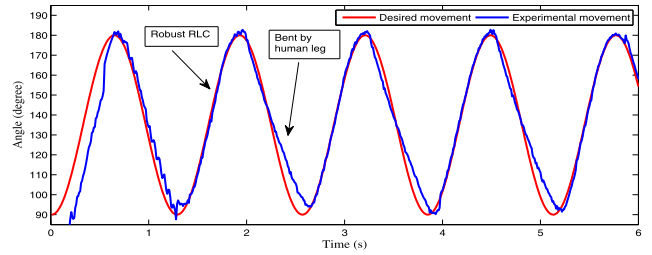


FIGURE 5. The output tracking profile of right knee.

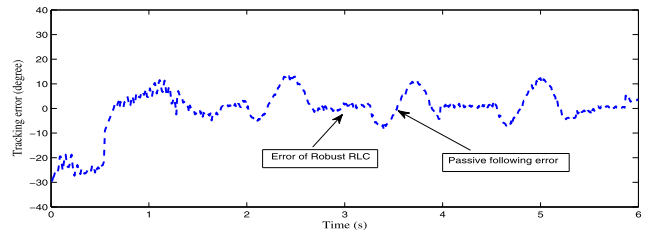


FIGURE 6. The tracking error profile of right knee.

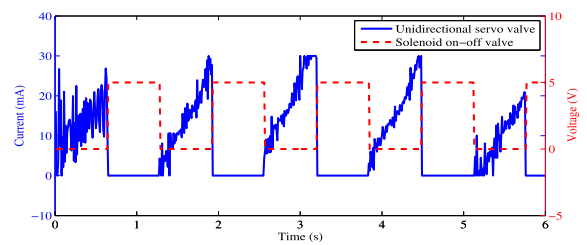


FIGURE 7. The control input profile of right knee.

C. RESULTS AND ANALYSIS

The controller is conducted in all the four actuated joints of the leg exoskeleton so as to verify the performance of the developed HHS and the energy saving control scheme. Owing to the similarity of the movement of two legs, only the profiles of the right one are shown here. Figs. 5 and 8 show the position tracking of the right knee and right hip, respectively. Figs. 6 and 9 demonstrate the corresponding tracking errors. In the tracking profiles, the first half cycle represents the movement in the stance phase, and the second half cycle represents the swing motion. In other words, in the stance phase, the exoskeleton legs are driven by the unidirectional servo valves of the HHS, and in the swing phase, the exoskeleton legs are released via the solenoid valves to follow the wearer’s movement.

From Figs. 5 and 8, we can see that in the stance phase the exoskeleton legs track the wearer’s movement successfully via the robust RLC after the first learning period. As the exoskeleton leg is bent by the human leg in the swing phase, the tracking errors of the second half cycle are larger than that of the first half.

The control inputs of the exoskeleton leg are shown in Fig. 7 and 10, from which we can see that the output current of the controller is well limited between 0 and 30 mA, and

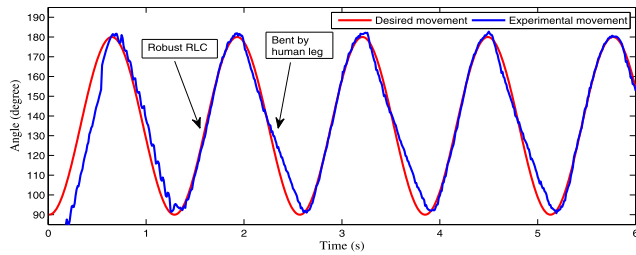


FIGURE 8. The output tracking profile of right hip.

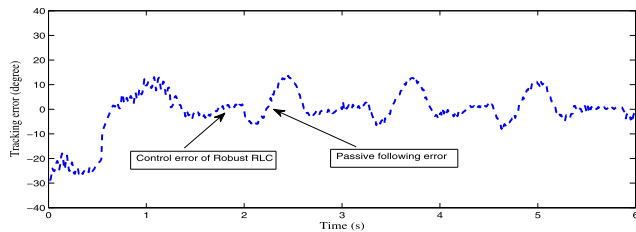


FIGURE 9. The tracking error profile of right hip.

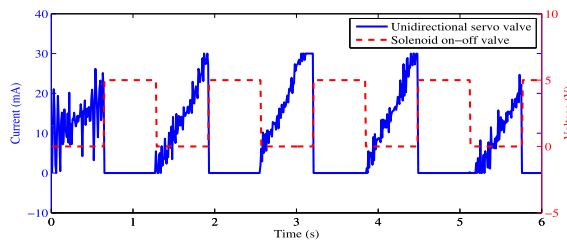


FIGURE 10. The control input profile of right hip.

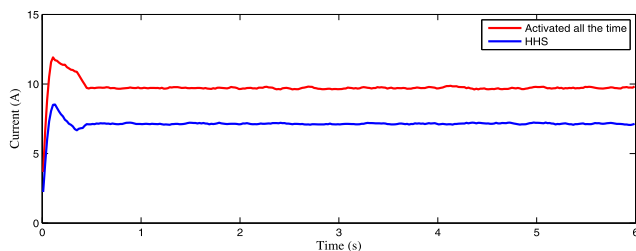


FIGURE 11. Comparison of power consumptions (electric current).

the unidirectional cylinders are controlled only in half of the walking cycle.

Further, the power consumption in the whole control process is shown in Fig. 11. Compared to the fully-driven hydraulic system that needs almost 10 Ampere current to drive the hydraulic pump, only 7 Ampere current is needed to make the pressure of the hydraulic pump stable when the proposed HHS is adopted. That is, the energy consumption will be decreased by 30% in experiment.

VI. CONCLUSION

In this paper, a novel control scheme is proposed for a leg exoskeleton driven by hybrid hydraulic system to achieve precise tracking and power consumption reduction. The hybrid

hydraulic system consists of a unidirectional servo valve and solenoid on-off valve, the unidirectional valve is controlled in the stance phase by introducing a robust repetitive learning control scheme under the assumption of periodic reference movement. The solenoid valve is activated in the swing phase to release the exoskeleton to follow the wearer's movement passively. By virtue of repetitive learning, the output tracking error of the leg exoskeleton in the stance phase can be reduced remarkably. Moreover, the power consumption of leg exoskeleton driven by the hybrid hydraulic system is almost 30% less than that of the system with bidirectional hydraulic system. Our next research phase is to investigate the energy saving control of the leg exoskeleton with non-repetitive reference movement.

REFERENCES

- [1] A. M. Dollar and H. Herr, "Lower extremity exoskeletons and active orthoses: Challenges and state-of-the-art," *IEEE Trans. Robot.*, vol. 24, no. 1, pp. 144–158, Feb. 2008.
- [2] W. Huo, S. Mohammed, J. C. Moreno, and Y. Amirat, "Lower limb wearable robots for assistance and rehabilitation: A state of the art," *IEEE Syst. J.*, vol. 10, no. 3, pp. 1068–1081, Sep. 2016.
- [3] H. Kawamoto and Y. Sankai, "Power assist method based on phase sequence and muscle force condition for HAL," *Adv. Robot.*, vol. 19, no. 7, pp. 717–734, Jan. 2005.
- [4] M. Talaty, A. Esquenazi, and J. E. Briceno, "Differentiating ability in users of the rewalk powered exoskeleton: An analysis of walking kinematics," in *Proc. IEEE Conf. Rehabil. Robot.*, Washington, DC, USA, Jun. 2013, pp. 1–5.
- [5] H. Kazerooni and R. Steger, "The Berkeley lower extremity exoskeleton," *J. Dyn. Syst. Meas. Control-Trans. ASME*, vol. 128, pp. 14–25, Mar. 2006.
- [6] E. Garcia, J. M. Sate, and J. Main, "Exoskeletons for human performance augmentation (EHPA): A program summary," *J. Robot. Soc. Jpn.*, vol. 20, no. 8, pp. 822–826, 2002.
- [7] R. Bogue, "Exoskeletons and robotic prosthetics: A review of recent developments," *Ind. Robot, Int. J.*, vol. 36, no. 5, pp. 421–427, Aug. 2009.
- [8] C. J. Walsh, K. Endo, and H. Herr, "A quasi-passive leg exoskeleton for load-carrying augmentation," *Int. J. Human. Robot.*, vol. 04, no. 03, pp. 487–506, Sep. 2007.
- [9] H. Kazerooni, A. Chu, and R. Steger, "That which does not stabilize, will only make us stronger," *Int. J. Robot. Res.*, vol. 26, no. 1, pp. 75–89, Jan. 2007.
- [10] J. E. Pratt, B. T. Krupp, C. J. Morse, B. T. Krupp, and C. J. Morse, "The RoboKnee: An exoskeleton for enhancing strength and endurance during walking," in *Proc. IEEE Int. Conf. Robot. Autom.*, New Orleans, LA, USA, Apr. 2004, pp. 2430–2435.
- [11] K. Suzuki, G. Mito, H. Kawamoto, Y. Hasegawa, and Y. Sankai, "Intention-based walking support for paraplegia patients with robot suit HAL," *Adv. Robot.*, vol. 21, no. 12, pp. 1441–1469, 2007.
- [12] K. Yamamoto, K. Hyodo, M. Ishii, and T. Matsuo, "Development of power assisting suit for assisting nurse labor," *JSME Int. J. Ser. C-Mech. Syst. Mach. Elements Manuf.*, vol. 45, no. 3, pp. 703–711, 2002.
- [13] K. Kong and D. Jeon, "Design and control of an exoskeleton for the elderly and patients," *IEEE/ASME Trans. Mechatronics*, vol. 11, no. 4, pp. 428–432, Aug. 2006.
- [14] B. Ugurlu, H. Oshima, and T. Narikiyo, "Lower body exoskeletons-supported compliant bipedal walking for paraplegics: How to reduce upper body effort?" in *Proc. IEEE Int. Conf. Robot. Autom.*, Hong Kong, May 2014, pp. 1354–1360.
- [15] X. Liu and K. H. Low, "Development and preliminary study of the NTU lower extremity exoskeleton," in *Proc. IEEE Conf. Cybern. Intell. Syst.*, Singapore, Dec. 2004, pp. 1243–1247.
- [16] C. Fleischer and G. Hommel, "Calibration of an EMG-based body model with six muscles to control a leg exoskeleton," in *Proc. IEEE Int. Conf. Robot. Autom.*, Roma, Italy, Apr. 2007, pp. 2514–2519.
- [17] Y. Yang, L. Ma, D. Huang, and N. Qin, "Output feedback repetitive learning control of electro-hydraulic actuator of lower limb rehabilitation exoskeleton," *Comput. Sci. Eng.*, vol. 21., no. 6, pp. 6–19, Oct. 2019.

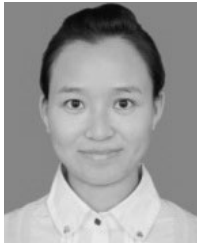
- [18] Z. Wang, S. Zhu, Q. Chen, X. Zhang, and Y. Song, "Sliding mode control of electro-hydraulic servo system for lower-limb exoskeleton based on RBF neural network," in *Proc. IEEE Conf. Ind. Electron. Appl.*, Auckland, New Zealand, Jun. 2015, pp. 79–83.
- [19] Z. Tang, D. Shi, D. Liu, Z. Peng, L. He, and Z. Pei, "Electro-hydraulic servo system for human lower-limb exoskeleton based on sliding mode variable structure control," in *Proc. IEEE Int. Conf. Inf. Autom.*, Yinchuan, China, Aug. 2013, pp. 559–563.
- [20] H. Kim, C. Seo, Y. J. Shin, J. Kim, and Y. S. Kang, "Locomotion control strategy of hydraulic lower extremity exoskeleton robot," in *Proc. IEEE Int. Conf. Adv. Intell. Mechatronics*, Busan, South Korea, Aug. 2015, pp. 577–582.
- [21] H. Kazerooni, J. Racine, L. Huang, and R. Steger, "On the control of the Berkeley lower extremity exoskeleton (BLEEX)," in *Proc. IEEE Int. Conf. Robot. Autom.*, Barcelona, Spain, Apr. 2005, pp. 4353–4360.
- [22] Z. Li, Y. Kang, Z. Xiao, and W. Song, "Human-robot coordination control of robotic exoskeletons by skill transfers," *IEEE Trans. Ind. Electron.*, vol. 64, no. 6, pp. 5171–5181, Jun. 2017.
- [23] C. Jarrett and A. J. Mcdaid, "Robust control of a cable-driven soft exoskeleton joint for intrinsic human-robot interaction," *IEEE Trans. Neural Syst. Rehabil. Eng.*, vol. 25, no. 7, pp. 976–986, Jul. 2017.
- [24] S. A. Murray, K. H. Ha, C. Hartigan, and M. Goldfarb, "An assistive control approach for a lower-limb exoskeleton to facilitate recovery of walking following stroke," *IEEE Trans. Neural Syst. Rehabil. Eng.*, vol. 23, no. 3, pp. 441–449, Mar. 2015.
- [25] B. Lee, H. Lee, J. Lee, K. Shin, J. Han, and C. Han, "Development of dynamic model-based controller for upper limb exoskeleton robot," in *Proc. IEEE Int. Conf. Robot. Autom.*, Saint Paul, MN, USA, May 2012, pp. 3173–3178.
- [26] W. Q. Xun, Z. K. Yu, and D. X. Dong, "An exoskeleton joint output force control technology based on improved ADRC," in *Proc. Int. Conf. Robot. Autom. Eng.*, Shanghai, China, 2017, pp. 146–150.
- [27] I. Jo and J. Bae, "Design and control of a wearable hand exoskeleton with force-controllable and compact actuator modules," in *Proc. IEEE Conf. Robot. Autom.*, Seattle, WA, USA, May 2015, pp. 5596–5601.
- [28] M. Chen, G. Tao, and B. Jiang, "Dynamic surface control using neural networks for a class of uncertain nonlinear systems with input saturation," *IEEE Trans. Neural Netw. Learn. Syst.*, vol. 26, no. 9, pp. 2086–2097, Sep. 2015.
- [29] V. Santibañez, K. Camarillo, J. Moreno-Valenzuela, and R. Campa, "A practical PID regulator with bounded torques for robot manipulators," *Int. J. Control Autom. Syst.*, vol. 8, no. 3, pp. 544–555, Jun. 2010.
- [30] M. Chen, B. Jiang, J. Zou, and X. Feng, "Robust adaptive tracking control of the underwater robot with input nonlinearity using neural network," *Int. J. Comput. Intell. Syst.*, vol. 3, no. 5, pp. 646–655, 2010.
- [31] J.-X. Xu, Y. Tan, and T.-H. Lee, "Iterative learning control design based on composite energy function with input saturation," *Automatica*, vol. 40, no. 8, pp. 1371–1377, Aug. 2004.
- [32] C. Wen, J. Zhou, Z. Liu, and H. Su, "Robust adaptive control of uncertain nonlinear systems in the presence of input saturation and external disturbance," *IEEE Trans. Autom. Control*, vol. 56, no. 7, pp. 1672–1678, Jul. 2011.
- [33] M. Chen, S. S. Ge, and B. Ren, "Adaptive tracking control of uncertain MIMO nonlinear systems with input constraints," *Automatica*, vol. 47, no. 3, pp. 452–465, Mar. 2011.
- [34] Z. Chen, Z. Li, and C. L. P. Chen, "Disturbance observer-based fuzzy control of uncertain MIMO mechanical systems with input nonlinearities and its application to robotic exoskeleton," *IEEE Trans. Cybern.*, vol. 47, no. 4, pp. 984–994, Apr. 2017.
- [35] Z. Li, C.-Y. Su, L. Wang, Z. Chen, and T. Chai, "Nonlinear disturbance observer-based control design for a robotic exoskeleton incorporating fuzzy approximation," *IEEE Trans. Ind. Electron.*, vol. 62, no. 9, pp. 5763–5775, Sep. 2015.
- [36] H. J. Asl, T. Narikiyo, and M. Kawanishi, "Neural network velocity field control of robotic exoskeletons with bounded input," in *Proc. IEEE Int. Conf. Adv. Intell. Mechatronics*, Munich, Germany, Jul. 2017, pp. 1363–1368.
- [37] S. Scalzi, S. Bifaretti, and C. M. Verrelli, "Repetitive learning control design for LED light tracking," *IEEE Trans. Control Syst. Technol.*, vol. 23, no. 3, pp. 1139–1146, May 2015.
- [38] M. Sun, S. Ge, and I. Mareels, "Adaptive repetitive learning control of robotic manipulators without the requirement for initial repositioning," *IEEE Trans. Robot.*, vol. 22, no. 3, pp. 563–568, Jun. 2006.
- [39] J.-X. Xu and R. Yan, "On repetitive learning control for periodic tracking tasks," *IEEE Trans. Autom. Control*, vol. 51, no. 11, pp. 1842–1848, Nov. 2006.
- [40] C. M. Verrelli, S. Pirozzi, P. Tomei, and C. Natale, "Linear repetitive learning controls for robotic manipulators by Padé approximants," *IEEE Trans. Control Syst. Technol.*, vol. 23, no. 5, pp. 2063–2070, Sep. 2015.
- [41] Y. Yang, L. Ma, and D. Huang, "Development and repetitive learning control of lower limb exoskeleton driven by electrohydraulic actuators," *IEEE Trans. Ind. Electron.*, vol. 64, no. 5, pp. 4169–4178, May 2017.
- [42] K. Zhou and D. Wang, "Digital repetitive learning controller for three-phase CVCF PWM inverter," *IEEE Trans. Ind. Electron.*, vol. 48, no. 4, pp. 820–830, Aug. 2001.
- [43] T. Manayathara, T.-C. Tsao, and J. Bentsman, "Rejection of unknown periodic load disturbances in continuous steel casting process using learning repetitive control approach," *IEEE Trans. Control Syst. Technol.*, vol. 4, no. 3, pp. 259–265, May 1996.
- [44] Y. Yang, D. Huang, and X. Dong, "Enhanced neural network control of lower limb rehabilitation exoskeleton by add-on repetitive learning," *Neurocomputing*, vol. 323, pp. 256–264, Jan. 2019.
- [45] D. Huang, J.-X. Xu, S. Yang, and X. Jin, "Observer based repetitive learning control for a class of nonlinear systems with nonparametric uncertainties," *Int. J. Robust Nonlinear Control*, vol. 25, no. 8, pp. 1214–1229, May 2015.
- [46] R. Lu, Z. Li, C.-Y. Su, and A. Xue, "Development and Learning Control of a Human Limb With a Rehabilitation Exoskeleton," *IEEE Trans. Ind. Electron.*, vol. 61, no. 7, pp. 3776–3785, Jul. 2014.
- [47] S. S. Ge, C. Hang, and L. Woon, "Adaptive neural network control of robot manipulators in task space," *IEEE Trans. Ind. Electron.*, vol. 44, no. 6, pp. 746–752, Dec. 1997.
- [48] H. E. Merritt, *Hydraulic Control Systems* New York, NY, USA: Wiley, 1967.
- [49] D. Won, W. Kim, D. Shin, and C. C. Chung, "High-gain disturbance observer-based backstepping control with output tracking error constraint for electro-hydraulic systems," *IEEE Trans. Control Syst. Technol.*, vol. 23, no. 2, pp. 787–795, Mar. 2015.
- [50] J.-X. Xu and R. Yan, "Synchronization of chaotic systems via learning control," *Int. J. Bifurcation Chaos*, vol. 15, no. 12, pp. 4035–4041, Dec. 2005.
- [51] F. Lewis, C. Abdallah, and D. Dawson, *Control of Robot Manipulators*. New York, NY, USA: MacMillan, 1993.



YONG YANG received the B.S. degree in mechatronic engineering, the M.S. degree in mechanical engineering, and the Ph.D. degree in control science and engineering from Southwest Jiaotong University, in 2011, 2013, and 2017, respectively. He is currently with the School of Electrical Engineering and Electronic Information, Xihua University, Chengdu, China. His current research interests include robotics, exoskeleton systems, learning control, adaptive control, and mechatronics system design.



XIUCHENG DONG was a Visiting Scholar with the Red River College, Canada, in 2000. In 2006, he was a Senior Visiting Scholar with Yamaguchi University, Japan. He is currently a Professor with the School of Electrical Engineering and Electronic Information, Xihua University, China. His research interests broadly involve the areas of intelligent control, modeling of nonlinear systems, machine vision, and virtual reality.



XIA LIU received the Ph.D. degree from the University of Electronic Science and Technology of China, in 2011. From 2009 to 2010, she was a Visiting Scholar with the Department of Electrical and Computer Engineering, University of Alberta, Canada. From 2013 to 2014, she was a Visiting Scholar with the Department of Mechanical Engineering, The University of Adelaide, Australia. Since 2012, she has been with the School of Electrical Engineering and Electronic Information, Xihua University, China, where she is currently a Professor. Her research interest includes nonlinear system and control, especially control of robotic teleoperation systems.



DEQING HUANG (Member, IEEE) received the B.S. and Ph.D. degrees in applied mathematics from the Mathematical College, Sichuan University, Chengdu, China, in 2002 and 2007, respectively, and the Ph.D. degree in control engineering from the National University of Singapore (NUS), Singapore, in 2011. He attended the Department of Electrical and Computer Engineering (ECE), NUS, in 2006. From January 2010 to February 2013, he was a Research Fellow with the Department of Electrical and Computer Engineering, NUS. From March 2013 to January 2016, he was a Research Associate with the Department of Aeronautics, Imperial College London, London, U.K. In January 2016, he joined the Department of Electronic and Information Engineering, Southwest Jiaotong University, Chengdu, China, as a Professor and the Head of the Department. His research interests are in the areas of modern control theory, artificial intelligence, fault diagnosis, and robotics.

• • •